Published May 13, 2016

Original Research

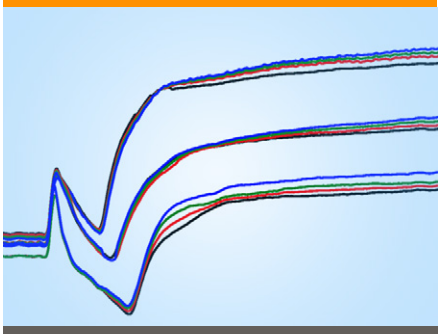

Core Ideas

- A TDR waveform interpretation method for NAPL content in soils was developed.
- Correlations between the dielectric response and the NAPL content were determined.
- The α dielectric mixing model for predicting NAPL presence in soils was expanded.
- This methodology can be used to obtain predictions of volumetric NAPL content.

Estimating Nonaqueous-Phase Liquid Content in Variably Saturated Soils Using Time Domain Reflectometry

Alessandro Comegna,* Antonio Coppola, Giovanna Dragonetti, and Angelo Sommella

In recent years, several studies have been conducted in the detection and observation of nonaqueous-phase liquids (NAPLs) in contaminated soils. Successful remediation of an NAPL-contaminated site requires appropriate characterization of both the plume extent and the soil volumetric NAPL content (θ_{NAPL}). Noninvasive geophysical techniques, such as time domain reflectometry (TDR), may be used to discriminate between θ_{NAPL} and soil volumetric water content (θ_w). Accordingly, the main aim of this work was to develop a TDR waveform interpretation method based on soil dielectric permittivity measurement and observation of the change in the reflected TDR signal amplitude at relatively long times from the waveform source. We demonstrated that the asymptotic value of the reflection signal coefficient can be univocally related with θ_{NAPL} in an unsaturated soil. In the procedure adopted, a new formulation of a dielectric mixing model was also derived, introducing a fourth phase that takes the NAPL presence into account. Multiple samples of sandy, silt loam, and loamy soils, at predetermined different θ_w and θ_{NAPL}, were tested, each test consisting in emitting a TDR signal to the soil sample and receiving and analyzing the reflected electromagnetic wave. An empirical dielectric mixing model was calibrated and implemented to estimate the θ_{NAPL}. Equipment calibration, measurement accuracy, and error sources, related both to the experimental procedure setup and to the sample preparation conditions, are discussed. The results show that the suggested methodology can be used to obtain predictions of volumetric NAPL content (θ_{NAPL}) with acceptable accuracy (R^2 = 0.95).

Abbreviations: EF, model efficiency; LNAPL, light nonaqueous-phase liquid; MAE, mean absolute percentage error; MBE, mean bias error; ME, maximum absolute percentage error; NAPL, nonaqueous-phase liquid; TDR, time domain reflectometry.

Nonaqueous-phase liquids (NAPLs) are organic compounds with low or no solubility in water. These pollutants are widely used in several human activities and can contribute to severe contamination of soils and groundwater aquifers. The existence of these dissolved organic contaminants in drinking water represents a risk for human health and the entire environment, even at low concentrations of a few parts per billion (Mohamed, 2006).

Classically, NAPLs can be subdivided into those that are denser than water (DNAPLs) and those that are lighter than water (LNAPLs). Chlorinated solvents such as trichloroethylene, tetrachloroethylene, and polychlorinated biphenyl oils are widespread examples of DNAPLs. Toluene, xylene, and hydrocarbon fuels such as gasoline, kerosene, and jet fuels are common LNAPL contaminants that pollute the environment extensively (Illangasekare, 1998; Jury and Horton, 2004).

The distribution of NAPLs in the ground can be very complex and may change with time. Following a near-surface release, NAPLs penetrate the subsurface as an immiscible pure oil phase that migrates in response to gravity and capillary forces. This results in substantial sensitivity to the local distribution of soil and aquifer properties (e.g., permeability and

A. Comegna and A. Coppola, School of Agricultural, Forestry, Food and Environmental Sciences (SAFE), Univ. of Basilicata, Potenza, Italy; G. Dragonetti, Mediterranean Agronomic Institute, Land and Water Division, IAMB, Bari 70010, Italy; and A. Sommella, Dep. of Agriculture, Univ. of Naples Federico II, Naples, Italy. *Corresponding author (alessandro.comegna@unibas.it).

Vadose Zone J.
doi:10.2136/vzj2015.11.0145
Received 6 Nov. 2015.
Accepted 21 Feb. 2016.

Vol. 15, Iss. 5, 2016

porosity) beneath the source (Gerhard et al., 2007). As a result, NAPL contamination in soils can follow two different patterns (Mercer and Cohen, 1990; Haridy et al., 2004; Francisca and Montoro, 2014): (i) immobile residuals, which refers to small and disconnected blobs or ganglia, and (ii) mobile pools, which indicates the presence of a connected-phase accumulated fluid above the groundwater.

Remediation of sites with contaminated soil requires accurate knowledge of the contaminant distribution in the soil profile and groundwater. Methods commonly used to characterize contaminated sites involve soil drilling, sampling, and the installation of monitoring wells for the collection of soil and water samples (Mercer and Cohen, 1990).

Given the cost of these technologies, other noninvasive techniques have been sought to extensively characterize sites and provide volume-averaged properties that support localized measurements provided by sampling and coring. Indirect detection with geophysical methods (e.g., radar, resistivity, and conductivity) offers an attractive alternative (Redman et al., 1991). In particular, the time domain reflectometry (TDR) technique has been proposed as potentially exhibiting sufficient sensitivity and lateral and vertical resolution for characterization of soil NAPL volumes. This is because commonly encountered NAPLs have a low dielectric permittivity of 2 to10 vs. 81 for water (Haridy et al., 2004). However, NAPL detection becomes difficult in the case of unsaturated soil at low water content due to the low dielectric permittivity of air (1) and soil mineral grains (3–7) (Alharthi et al., 1986; Ajo-Franklin et al., 2006).

Most studies have demonstrated the potential of the TDR technique in estimating NAPL presence in saturated soils (Redman and DeRyck, 1994; Chenaf and Amara, 2001; Haridy et al., 2004; Mohamed and Said, 2005; Moroizumi and Sasaki, 2008). Few experiments have been conducted on unsaturated soils (Persson and Berndtsson, 2002; Rinaldi and Francisca, 2006; Francisca and Montoro, 2012). In these studies, the estimation of NAPLs using TDR measurements of dielectric properties has relied greatly on various mixing models relating the measured dielectric permittivity to the volume fractions of the pore fluids and various soil phases such as solid, water, air, and NAPLs (van Dam et al., 2005).

From a physical point of view, the presence of NAPLs in soil contributes to complicate transport equations and interpretative dielectric models because a new phase is introduced, which furthermore can be liquid (immiscible and dissolved) and volatile.

Some interesting results have been achieved by, among others, Persson and Berndtsson (2002) while investigating the influence of different LNAPLs (sunflower seed oil, a synthetic motor oil, and an *n*-paraffin oil) on TDR measurements in a homogeneous silica sand under saturated and unsaturated soil conditions. Measurements of both dielectric permittivity and electrical conductivity allowed a method to be developed (a two-step method) that measured the dielectric properties of the system against the amount of NAPL in the soils. However, the approach requires detailed calibration data for dielectric permittivity and electrical conductivity relationships on a wide range of NAPL concentrations, which restricts the applicability of the method to laboratory-controlled experiments in homogeneous materials.

Haridy et al. (2004) conducted a series of laboratory experiments with NAPLs. They compared their results with those obtained by Persson and Berndtsson (2002) and concluded that the two-step approach was not applicable in the fine sand used in their experiment due to the fact that no correlation was observed between the amount of NAPL in the soil and the electrical conductivity.

Rinaldi and Francisca (2006) and Francisca and Montoro (2012) used a coaxial impedance dielectric reflectometry technique to measure the complex dielectric permittivity in sands contaminated by a paraffin oil. They observed the dielectric response of the NAPL-contaminated soils and provided a method for NAPL estimation by coupling a mixing model and the complex dielectric response of contaminated soils of different texture. The limit of this approach, and in general of the approaches described above, is that it requires calibration curves relating the dielectric permittivity and the volumes of fluids θ_f (= water + NAPL) to be built for specific soil texture and porosity conditions.

There is thus a need for a more general calibration procedure for the application of the TDR technique to any soil type, porous system, and different water saturation conditions. To partially fill the gap, in this study we performed a series of laboratory-controlled experiments aiming to extend the above research on TDR identification of organic-contaminated soils by the amplitude of the reflected signal combined with dielectric permittivity measurements. Specific aims included: (i) calibration and validation of a dielectric mixing model (α model) in the form proposed by Francisca and Montoro (2012) for predicting the dielectric permittivity of NAPL-contaminated soils, and (ii) development of a general methodology for evaluating the correlations between the dielectric response and the NAPL content in variably saturated soils with different textures and pedological characteristics.

Theoretical Background and Operational Principles of TDR

The TDR technique is a widely accepted geophysical method to measure the dielectric permittivity of liquids and solids described by a complex number, ε_r^*, which is written as (Robinson and Friedman, 2002)

$$\varepsilon_r^* = \varepsilon_r' - J\left(\varepsilon_r'' + \frac{\sigma}{\omega\varepsilon_0}\right) \quad [1]$$

where ε_r' is the real part of the dielectric permittivity, which accounts for the energy stored in the dielectrics at a given frequency

and temperature, ε_r'' is the imaginary part due to relaxations, σ (S m^{-1}) is the zero-frequency conductivity, ω is the angle frequency, $J = \sqrt{-1}$ is the imaginary number, and ε_0 (= 8.85 × 10^{-12} F m^{-1}) is the permittivity in free space.

At the highest effective frequency of a TDR cable tester (200 MHz–1.5 GHz) where the dielectric losses can be assumed to be negligible, using a waveguide (or probe) of known length L, the apparent dielectric permittivity ε_a ($\cong$ the real part of the permittivity) is measured from the propagation velocity v (= $2L/t$) of an electromagnetic wave along the waveguide through the soil by

$$\varepsilon_a = \left(\frac{c}{v}\right)^2 \quad [2]$$

where c (= 3 × 10^8 m s^{-1}) is the velocity of an electromagnetic wave in a vacuum (Topp et al., 1980) and t is the travel time, which represents the time that is needed by the TDR signal to travel back and forth to the waveguide of length L (m) and can be written as

$$t = \frac{2L}{c}\sqrt{\varepsilon_a} \quad [3]$$

Equation [3] yields the direct dependence between the travel time t of the signal and the soil dielectric properties (i.e., ε_a).

Dielectric Mixing Models

Dielectric mixing models have been developed to estimate the apparent dielectric permittivity of a multiphase medium (Hilhorst, 1998; Regalado et al., 2003; Comegna et al., 2013a). In their classical application, these models approach an uncontaminated soil as a mixture of three (e.g., soil, water, and air) or four (e.g., soil, free water, bound water, and air) dielectric phases and relate the composite dielectric permittivity of the medium, ε_a, to the dielectric permittivity of each individual phase. Recently these models have been extended to determine apparent dielectric properties of NAPL-contaminated soils (Persson and Berndtsson, 2002; Francisca and Montoro, 2012; Comegna et al., 2013b).

Among the many physical models of dielectric permittivity available in the literature (among others, De Loor, 1954; Dobson et al., 1985; Regalado et al., 2003), in this study we opted for the so-called exponential α model (Birchak et al., 1974; Roth et al., 1990; Hilhorst, 1998):

$$\varepsilon_a^\alpha = \sum_{i=1}^{n} V_i \varepsilon_i^\alpha \quad [4]$$

where ε_a is the apparent dielectric permittivity of the mixture, V_i and ε_i are the volume and the permittivity, respectively, of each component; the exponent α is a curve-fitting parameter that ranges between −1 and 1 and may be correlated with the internal structure of the medium. From a physical point of view, α is a geometric factor relating the direction of the effective layering of the different dielectric components to the direction of the applied electrical field (Hilhorst, 1998). It has been widely suggested (Dobson et al., 1985; Alharthi et al., 1986; Roth et al., 1990; Huisman et al., 2003) that α is equal to 0.5 for isotropic and homogeneous soils, but in general it is a fitting parameter and cannot be measured directly or inferred from other soil properties. However, despite this limitation and the apparent simplicity of using the α mixing model, remarkably good agreement was found in modeling the dielectric properties of geological materials (Knight, 2001) and soil–water–NAPL mixtures (Francisca and Montoro, 2012; Comegna et al., 2013a, 2013b).

For mixtures of soil saturated with water, the α model yields (Rinaldi and Francisca; 2006):

$$\varepsilon_{sw}^\alpha = \left[(1-\phi)\varepsilon_s^\alpha + \phi S \varepsilon_w^\alpha + \phi(1-S)\varepsilon_{air}^\alpha\right] \quad [5]$$

where ε_{sw} is the permittivity of the soil–water mixture; ε_s, ε_w, and ε_{air} are the permittivities of soil particles, water, and air, respectively; S is the effective water saturation; and ϕ is the porosity of the sample. Similarly for soil–organic mixtures, the α model becomes

$$\varepsilon_{sNAPL}^\alpha = \left[(1-\phi)\varepsilon_s^\alpha + \phi S \varepsilon_{NAPL}^\alpha + \phi(1-S)\varepsilon_{air}^\alpha\right] \quad [6]$$

where ε_{sNAPL} is the permittivity of the soil–NAPL compound, and ε_{NAPL} is the NAPL permittivity. A medium composed of soil particles, water, NAPL, and air can be considered as a mixture of soil, water, and air (Eq. [5]) with soil, NAPL, and air (Eq. [6]):

$$\varepsilon_a^\alpha = \left[\beta \varepsilon_{sNAPL}^\alpha + (1-\beta)\varepsilon_{sw}^\alpha\right] \quad [7]$$

where β is the relative volume of NAPL in water:

$$\beta = \frac{\theta_{NAPL}}{\theta_w + \theta_{NAPL}} = \frac{\theta_{NAPL}}{\theta_f} \quad [8]$$

where θ_f is the volumetric fluid content (cm^3 cm^{-3}), the sum of the volumetric water content (θ_w) and the volumetric NAPL content (θ_{NAPL}); β ranges between 0 (soil–water mixtures) and 1 (soil–NAPL mixtures).

Estimating Volumetric NAPL Content in Variably Saturated Soils

To overcome the difficulties and limitations related to NAPL estimation in complex systems (i.e., with three or four phases) by means of TDR, we now introduce and describe a methodology based on a new TDR waveform analysis approach, combined with the capability of the semi-empirical α mixing model.

The presence of an organic contaminant in soils is known to affect the dielectric permittivity of the porous medium (Persson and Berndtsson, 2002; Mohamed, 2006; Francisca and Montoro, 2012, Zhan et al., 2013; Comegna et al., 2013b). In general, in a partly

saturated, contaminated soil, for a constant volumetric water content (θ_w), the dielectric permittivity (ε_a) of the medium decreases as θ_{NAPL} increases due to the low dielectric permittivity values (compared with that of water) that most NAPLs exhibit (Persson and Berndtsson, 2002). This is a starting point for understanding the influence of NAPLs on TDR measurements but does not entirely explain the dielectric behavior of an NAPL-contaminated soil. The main difficulties in θ_{NAPL} evaluation via TDR can be summarized as follows:

1. The TDR technique supplies the dielectric permittivity of the medium in terms of "global response," which means that ε_a depends on the total volume of the distinct phases involved (including NAPL). Therefore TDR cannot directly discriminate the presence of NAPL.

2. The dielectric permittivity of most common NAPLs is similar to that of mineral particles. As a consequence, under certain conditions (e.g., at low water content), NAPL presence may be confused with the dielectric response of a dry soil.

3. The relationship between the dielectric permittivity of the contaminated soil and θ_{NAPL} is not univocal, in the sense that a given observed permittivity corresponds to different volumetric combinations of water and NAPL (i.e., different θ_f). Thus, even if both ε_a and θ_w are available, θ_{NAPL} cannot be inferred without additional information on the distribution of the fluid phase in the soil (see Persson and Berndtsson, 2002).

Looking at Eq. [5–8], it is evident that NAPL determination in soils is constrained by the knowledge of the volumetric fluid content (θ_f), the relative volume of NAPL in water (β), and of course the dielectric permittivity of the contaminated medium (ε_a). A priori knowledge of θ_f and β is not possible because both depend on the unknown θ_{NAPL}. The classical TDR approach for water content estimation is commonly based on the analysis of the signal characteristics in the time interval between the first peak (t_1) and the reflection point (t_2) corresponding to the end of the transmission line. In the presence of NAPLs, the waveform information included in the time domain $t_1 \le t \le t_2$ may be used to detect NAPL occurrence but not its volumetric content.

To overcome these difficulties, we suggest a general methodology to relate the dielectric permittivity to the volumes of organic contaminants in soils by analyzing the TDR signal attenuation in an observation window wide enough to include the multiple reflections that can generally be found on a TDR waveform at long times (and thus distances) from the waveform source, a technique similar to that used to estimate the electrical conductivity of the bulk soil (Giese and Tiemann, 1975; Rhoades et al., 1976; Dalton et al., 1984). At long travel times, when multiple reflections have died out, the amplitude of the reflection coefficient tends to stabilize and the final value (ρ_f), combined with the corresponding measure of the dielectric permittivity, can be utilized to estimate the volumetric NAPL content. Since, for a fixed combination of θ_{NAPL} and θ_w, the magnitude of the signal at long travel times is influenced by the soil porosity ϕ (see, for example, Jung et al., 2013), in the proposed approach ϕ was kept constant throughout all tests.

To predict θ_{NAPL} with the proposed technique, the dielectric α mixing model needs a new formulation. First, Eq. [7] is reformulated in terms of β:

$$\beta = \frac{\varepsilon_{sw}^{\alpha} - \varepsilon_a^{\alpha}}{\varepsilon_{sw}^{\alpha} - \varepsilon_{sNAPL}^{\alpha}} = \frac{\left[(1-\phi)\varepsilon_s^{\alpha} + \phi S\varepsilon_w^{\alpha} + \phi(1-S)\varepsilon_{air}^{\alpha}\right] - \varepsilon_a^{\alpha}}{\left[(1-\phi)\varepsilon_s^{\alpha} + \phi S\varepsilon_w^{\alpha} + \phi(1-S)\varepsilon_{air}^{\alpha}\right] - \left[(1-\phi)\varepsilon_s^{\alpha} + \phi S\varepsilon_{NAPL}^{\alpha} + \phi(1-S)\varepsilon_{air}^{\alpha}\right]} \quad [9]$$

Substituting Eq. [8] into Eq. [9], θ_{NAPL} can be calculated as

$$\theta_{NAPL} = \frac{(1-\phi)\varepsilon_s^{\alpha} + \phi\varepsilon_{air}^{\alpha} + \theta_f\left(\varepsilon_w^{\alpha} - \varepsilon_{air}^{\alpha}\right) - \varepsilon_a^{\alpha}}{\varepsilon_w^{\alpha} - \varepsilon_{NAPL}^{\alpha}} \quad [10]$$

Equation [10] describes the dependence of θ_{NAPL} on ϕ and θ_f.

Now, for a given ε_a value, we found that the following empirical linear relationship between volumetric fluid content and the final value of the reflection coefficient ρ_f,

$$\theta_f = a\rho_f + b \quad [11]$$

can be assumed to describe the functional dependence of θ_f vs. ρ_f. Below, we show that the slope coefficient a may be assumed constant for a selected soil ($a = a_c$ = constant), whereas the intercept b can be related to the dielectric permittivity by

$$b = b_1\varepsilon_a^2 + b_2\varepsilon_a + b_3 \quad [12]$$

where b_1, b_2, and b_3 are fitting parameters of a second-order polynomial equation. As a result, θ_f can be written as

$$\theta_f = a_c\rho_f + \left(b_1\varepsilon_a^2 + b_2\varepsilon_a + b_3\right) \quad [13]$$

and finally, Eq. [10] and [13] may be combined to yield

$$\theta_{NAPL} = \frac{(1-\phi)\varepsilon_s^{\alpha} + \phi\varepsilon_{air}^{\alpha}}{\varepsilon_w^{\alpha} - \varepsilon_{NAPL}^{\alpha}} + \frac{\left[a_c\rho_f + \left(b_1\varepsilon_a^2 + b_2\varepsilon_a + b_3\right)\right]\left(\varepsilon_w^{\alpha} - \varepsilon_{air}^{\alpha}\right) - \varepsilon_a^{\alpha}}{\varepsilon_w^{\alpha} - \varepsilon_{NAPL}^{\alpha}} \quad [14]$$

Equation [14] allows the volumetric NAPL content to be estimated once ε_a and ρ_f are estimated from the TDR waveform analysis.

Materials and Methods

Materials and Properties

The soils investigated in this study were a sandy Vitric Andosol (IUSS Working Group WRB, 2006), a silty loam Anthrosol

(IUSS Working Group WRB, 2006), and a loam Haplic Luvisol (IUSS Working Group WRB, 2006), all located in southern Italy.

The soil texture was determined using hydrometer and sieving analysis (Day, 1965); soil organic C content was analyzed according to the Walkley–Black method as described by Allison (1965); the soil solution electrical conductivity (EC_w) was measured with the method proposed by Miller and Curtin (2006), while the soil pH was determined using a 1:1 soil/water ratio (Eckert, 1988). The results of this analysis are presented in Table 1.

Table 1. Main physicochemical properties of the soils.

Soil	Depth	Soil texture and classification (USDA)				Porosity	Organic C	EC_w†	pH
		Sand	Clay	Silt	Texture				
	cm	——% ——				——% ——		dS m^{-1}	
Vitric Andosol	0–20	80.0	8.0	12.0	sand	0.56	1.90	0.80	7.30
Anthrosol	0–20	15.7	11.6	72.7	silt loam	0.57	1.84	0.17	8.37
Haplic Luvisol	0–20	41.4	16.4	42.2	loam	0.52	0.30	0.13	8.40

† Soil solution electrical conductivity.

Because the density of the NAPL (corn oil: $\varepsilon_{NAPL} = 3.2$) used as soil contaminant is 0.905 g cm^{-3} (at 25°C), it belongs to the LNAPLs. The electrical conductivity of the water used was 0.0005 dS m^{-1}.

Experimental Setup

The experimental setup consisted of a TDR unit constituted by a signal generator (Tektronix 1502C cable tester) and a three-wire TDR probe, with 14.5-cm-long waveguides connected to the tester by a 2-m-long coaxial cable. The reflected signals are collected by a PC-based data acquisition–processing system. A MATLAB code based on the method of Baker and Allmaras (1990) was then developed for post-processing the acquired TDR signals. Figure 1 shows the dielectric measurement system used in the experiments.

Experimental Design, Sampling Properties, and Testing Procedures

Two groups of experiments (referred to below as Exp. 1 and Exp. 2) were performed in a laboratory on soil samples collected from the Ap horizon of the soils under study. Experiment 1 refers to dielectric permittivity measurements conducted on soil mixtures with known different θ_w and θ_{NAPL}. Further, in the procedure adopted, β and θ_f were varied from 0 to 1 (with steps of 0.25) and from 0.05 to 0.50 (by 0.05 increments), respectively, to achieve different levels of soil contamination. For each mixture, the ε_a of the system was measured and the acquired data series were utilized for calibrating the α model.

On the basis of the results obtained from Exp. 1, in Exp. 2 we prepared NAPL-contaminated samples by varying β and ε_a. The volumetric fluid content θ_f and thus the water and NAPL volumes, for the soil mixtures were obtained via the α model (Eq. [7]). For all samples, TDR signals were acquired at two observation windows: (i) $t \cong 25$ ns and (ii) $t \cong 507$ ns.

For both Exp. 1 and 2, the soil samples were oven dried at 105°C and sieved at 2 mm. By following the procedure of Persson and Berndtsson (2002), known amounts of soil, water, and oil were mixed together, shaken, and then kept for 24 h in sealed plastic bags to avoid any evaporation. During this time, to ensure a uniform distribution of oil and water within the sample and good oil and water adsorption by the soil matrix, the soil mixture was stirred frequently. The soil was then placed in cylindrical polyvinyl chloride containers (15 cm high and 9.5 cm in diameter) in several steps during which it was carefully compacted until a 1.16 g cm^{-3} (Vitric Andosol), 1.13 g cm^{-3} (Anthrosol), and 1.27 g cm^{-3} (Haplic Luvisol) bulk density was attained. At each step, the compacted surface was scraped to prevent soil stratification. Soil samples were kept at a fairly constant temperature of 25°C during the TDR measurements using a thermostat box.

After packing, a TDR probe was inserted vertically into the soil. To avoid any difference in TDR readings (which may be generated, as is well known, by dissimilar geometric characteristics of the probe) all the measurements (Exp. 1 and 2) were made with the same TDR probe. Overall, for each soil, there were 50 (Exp. 1) and 20 (Exp. 2) NAPL-contaminated soil samples used for a full factorial analysis as presented in Tables 2 and 3, respectively. Furthermore, for each tested soil, an independent validation data set (50 soil samples for Exp. 1 and 20 for Exp. 2) was prepared for model validation. In each mixture of soil, water, and oil, 10 measurements were taken and averaged immediately after packing.

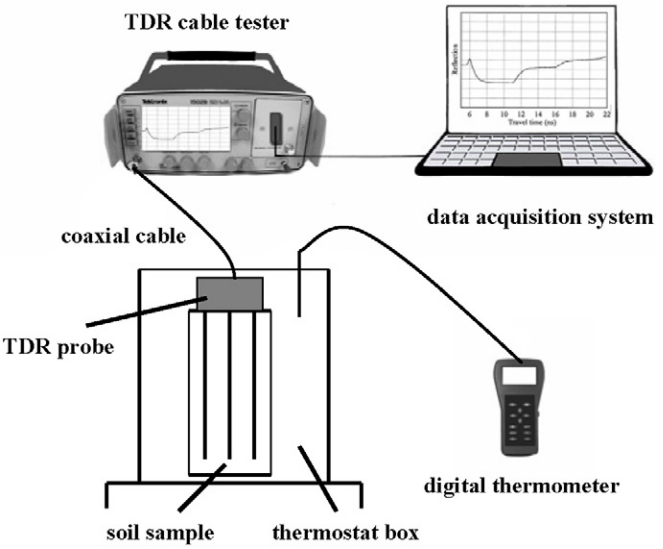

Fig. 1. Experimental setup used in nonaqueous-phase liquid experiments using time domain reflectometry (TDR).

Statistical Analysis

Statistical Indices for Model Performance Evaluation

Performance of the models (Eq. [7] and [14]) was evaluated by calculating: (i) the mean bias error (MBE), (ii) the model efficiency (EF), (iii) the maximum absolute percentage error (ME), and (iv) the mean absolute percentage error (MAE) statistical indices, computed according to the following relations (Legates and McCabe, 1999; Goovaerts et al., 2005):

$$\mathrm{MBE}=\frac{\sum_{i=1}^{N}(E_i-O_i)}{N}$$

$$\mathrm{EF}=1-\frac{\sum_{i=1}^{N}(E_i-O_i)^2}{\sum_{i=1}^{N}(O_i-\bar{O})^2}$$

$$\mathrm{ME}(\%)=\max\left|E_i-O_i\right|\times 100$$

$$\mathrm{MAE}(\%)=\frac{\left|E_i-O_i\right|}{N}\times 100$$

where E_i is the prediction (model-simulated data), O_i is the true value (observed data), $\bar{O}$ is the mean of the observed data, and N is the number of observations.

The MBE is a measurement of bias between the predicted and observed values: MBE = 0 means a perfect agreement between expected and observed data, and positive values indicate an average underprediction and vice versa. Parameter EF is an overall measure of the model's ability to predict the measured water content (EF = 1 means a perfect agreement between expected and observed values); ME and MAE express the maximum and the mean absolute difference observed between measured and expected values. For an ideal prediction, the values of ME and MAE should be 0.

Table 2. Combinations of moisture volume (V_w) and NAPL volume (V_{NAPL}) for determined levels of contamination (β) at different total fluid volumes (θ_f) and a fixed soil porosity (Exp. 1).

θ_f	Fluid volume	β = 1	β = 0.75	β = 0.50	β = 0.25	β = 0
$cm^3\ cm^{-3}$				cm^3		
0.05	V_w	0	13	27	40	53
	V_{NAPL}	53	40	27	13	0
0.10	V_w	0	27	53	80	106
	V_{NAPL}	106	80	53	27	0
0.15	V_w	0	40	80	120	159
	V_{NAPL}	159	120	80	40	0
0.20	V_w	0	53	106	159	213
	V_{NAPL}	213	159	106	53	0
0.25	V_w	0	66	133	199	266
	V_{NAPL}	266	199	133	66	0
0.30	V_w	0	80	159	239	319
	V_{NAPL}	319	239	159	80	0
0.35	V_w	0	93	186	279	372
	V_{NAPL}	372	279	186	93	0
0.40	V_w	0	106	213	319	425
	V_{NAPL}	425	319	213	106	0
0.45	V_w	0	120	239	359	478
	V_{NAPL}	478	359	239	120	0
0.50	V_w	0	133	266	399	532
	V_{NAPL}	532	399	266	133	0

Estimation of the Parameters of the Parallel Regression Lines θ_f vs. ρ_f

The methodology developed in this study requires statistical analysis of the relationship between the volumetric fluid content θ_f and the final reflection coefficient ρ_f to determine the coefficients a_c, b_1, b_2, and b_3 of Eq. [14]. The analysis was performed using analysis of covariance (ANCOVA) (at a significance level of 0.05), which is a statistical tool used to test the main and interaction effects of

Table 3. Combinations of volumetric fluid content (θ_f) and nonaqueous-phase liquid (NAPL) volume (V_{NAPL}) for different levels of contamination (β) and apparent dielectric permittivity (ε_a) values and a fixed soil porosity (Exp. 2).

	Vitric Andosol					Anthrosol					Haplic Luvisol				
Parameter	ε_a					ε_a					ε_a				
β	4	0.25	0.45	0.50	0.75	6	0.35	0.50	0.60	0.70	5.3	0.25	0.50	0.60	0.70
θ_f, $cm^3\ cm^{-3}$		0.120	0.150	0.165	0.265		0.205	0.285	0.355	0.415		0.165	0.230	0.280	0.345
V_{NAPL}, cm^3		32	72	88	211		76	151	226	309		44	122	178	257
β	5.5	0.25	0.50	0.60	0.75	7	0.30	0.40	0.50	0.60	7	0.15	0.25	0.50	0.65
θ_f, $cm^3\ cm^{-3}$		0.190	0.260	0.290	0.415		0.245	0.290	0.337	0.395		0.205	0.225	0.320	0.425
V_{NAPL}, cm^3		50	138	185	331		78	123	179	252		33	60	170	294
β	7	0.25	0.40	0.50	0.65	10	0.25	0.50	0.60	0.65	8.5	0.20	0.30	0.50	0.55
θ_f, $cm^3\ cm^{-3}$		0.245	0.300	0.335	0.435		0.320	0.350	0.410	0.460		0.230	0.265	0.335	0.355
V_{NAPL}, cm^3		65	128	178	301		85	186	261	318		50	85	178	208
β	10	0.10	0.30	0.45	0.50	12	0.20	0.30	0.40	0.50	12	0.10	0.20	0.30	0.40
θ_f, $cm^3\ cm^{-3}$		0.290	0.355	0.410	0.465		0.330	0.405	0.432	0.460		0.280	0.315	0.350	0.400
V_{NAPL}, cm^3		31	113	174	247		70	129	183	244		30	67	112	170
β	12	0.10	0.30	0.35	0.40	17	0.10	0.18	0.25	0.35	14	0.10	0.18	0.25	0.40
θ_f, $cm^3\ cm^{-3}$		0.345	0.425	0.455	0.480		0.420	0.460	0.490	0.550		0.320	0.350	0.375	0.455
V_{NAPL}, cm^3		37	136	169	204		45	88	130	205		34	67	100	193

categorical variables on a continuous dependent variable, controlling for the effects of selected other continuous variables that co-vary with the dependent variable. Thus, the ANCOVA analysis combines regression analysis and analysis of variance, providing for each soil investigated a way of statistically controlling the parallelism of the empirical linear relationships θ_f–ρ_f observed at different levels of soil contamination.

Briefly, in the standard ANCOVA analysis used for our purposes, for each soil two random variables θ_f and ρ_f of size $n = 4$ were drawn from each of $k = 5$ populations and were analyzed with respect to possible differences in the distribution of the so-called response variable, which is θ_f.

The equation commonly used and suitably adapted to the problem in context (Conover and Iman, 1982) is

$$\theta_{f\,ij} = b_{0\,j} + a_{1\,j}\rho_{f\,ij} + \varepsilon_{ij}, \quad i = 1, 2, \ldots, n \text{ and } j = 1, 2, \ldots, k$$

where a_{0j} and b_{1j} are the slopes and intercepts of k distinct linear regressions, and the residuals ε_{ij} are independent and normally distributed. The ANCOVA proceeds by testing for the equality of the slopes of these regression lines under the usual null hypothesis H_0: $a_{11} = a_{12} = \ldots = a_{1j}$, (i.e., the linear regressions have equal slopes but different intercepts), which is tested against the alternative hypothesis H_1: $a_{1j} \neq a_{1\zeta}$ for $j \neq \zeta = 1, 2, \ldots, k$.

Results and Discussion

Model Calibration and Validation

For the model (Eq. [7]) calibration procedure, permittivity values of the solid phase (ε_s) of 5.70, 3.70, and 3.57 were adopted (i.e., for the Vitric Andosol, Anthrosol, and Haplic Luvisol, respectively). They were measured with the immersion method, which is commonly used for measuring the ε_s of soils (Robinson and Friedman, 2002; Kameyama and Miyamoto, 2008; Comegna et al., 2013a; Coppola et al., 2013). The α parameter of the mixing model was then determined by an optimization procedure based on the least-square technique.

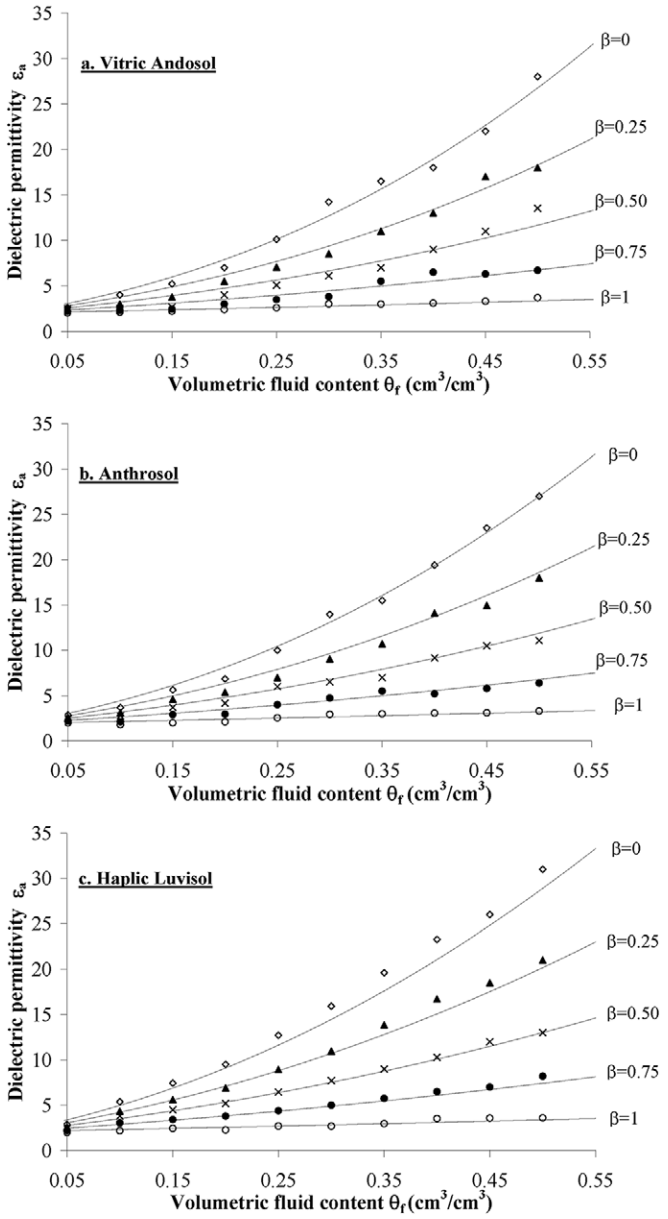

Fig. 2. Effect of volumetric fluid content (θ_f) on the dielectric permittivity (ε_a) of soil-water–nonaqueous-phase liquid (NAPL)–air mixtures at different levels of contamination (β): (a) Vitric Andosol, (b) Anthrosol, and (c) Haplic Luvisol.

In Fig. 2, the results of model validation are reported, and the measured ε_a (symbols) are shown as a function of θ_f for the fully uncontaminated soil ($\theta_f = \theta_w$: $\beta = 0$), the fully contaminated soil ($\theta_f = \theta_{NAPL}$: $\beta = 1$), and the soil at different degrees of contamination ($\theta_f = \theta_w + \theta_{NAPL}$: $\beta = 0.25$, 0.50, and 0.75). Dashed lines are the estimated (Eq. [7]) dielectric permittivities for different θ_f.

Table 4. Optimized α model parameter values and mean bias error (MBE) and model efficiency (EF) statistical indices at different levels of contamination (β) for Eq. [7].

		MBE					EF				
Soil	α	$\beta = 1$	$\beta = 0.75$	$\beta = 0.50$	$\beta = 0.25$	$\beta = 0$	$\beta = 1$	$\beta = 0.75$	$\beta = 0.50$	$\beta = 0.25$	$\beta = 0$
Vitric Andosol	0.40	−0.029	0.122	0.200	0.406	0.050	0.99	0.99	1.00	1.00	1.00
Anthrosol	0.45	−0.013	0.007	0.017	0.159	−0.340	1.00	1.00	1.00	1.00	1.00
Haplic Luvisol	0.50	−0.041	−0.210	−0.145	−0.487	−1.145	0.98	1.00	1.00	1.00	1.00

Figure 2 shows that dielectric permittivity increases with increasing θ_f, with the slope increasing as the β value decreases. Table 4 summarizes the values of the α parameter as well as the statistical indices used to compare the goodness of fit of the mixing model to the data. For each soil, the values of MBE and EF demonstrate the suitability of the α mixing model to describe the dielectric permittivity of soil with high accuracy in the θ_f range 0.05 to 0.50.

Nonaqueous-Phase Liquid Estimation in Variably Saturated Soils

Figure 3 shows the TDR waveforms obtained in the three tested soils. Recall that the TDR waveforms were acquired in two different time domains (t = 25.37 ns and t = 507.42 ns), using three selected groups of soil samples containing various combinations of water and oil. For a given soil, an ensemble of TDR traces was obtained by varying β and ε_a according to the procedure described above.

Further, Fig. 3a, 3c, and 3e show that in the time range t_1 – t_2 (i.e., between the first peak and the reflection point), TDR signals practically overlap, thus indicating equivalent travel times and permittivities. In this sense, the graphs show how analyzing the waveforms in the usual range t_1 to t_2 does not allow discrimination at all between oil and water volumetric contents. However, at times larger than t_2, TDR waveforms start

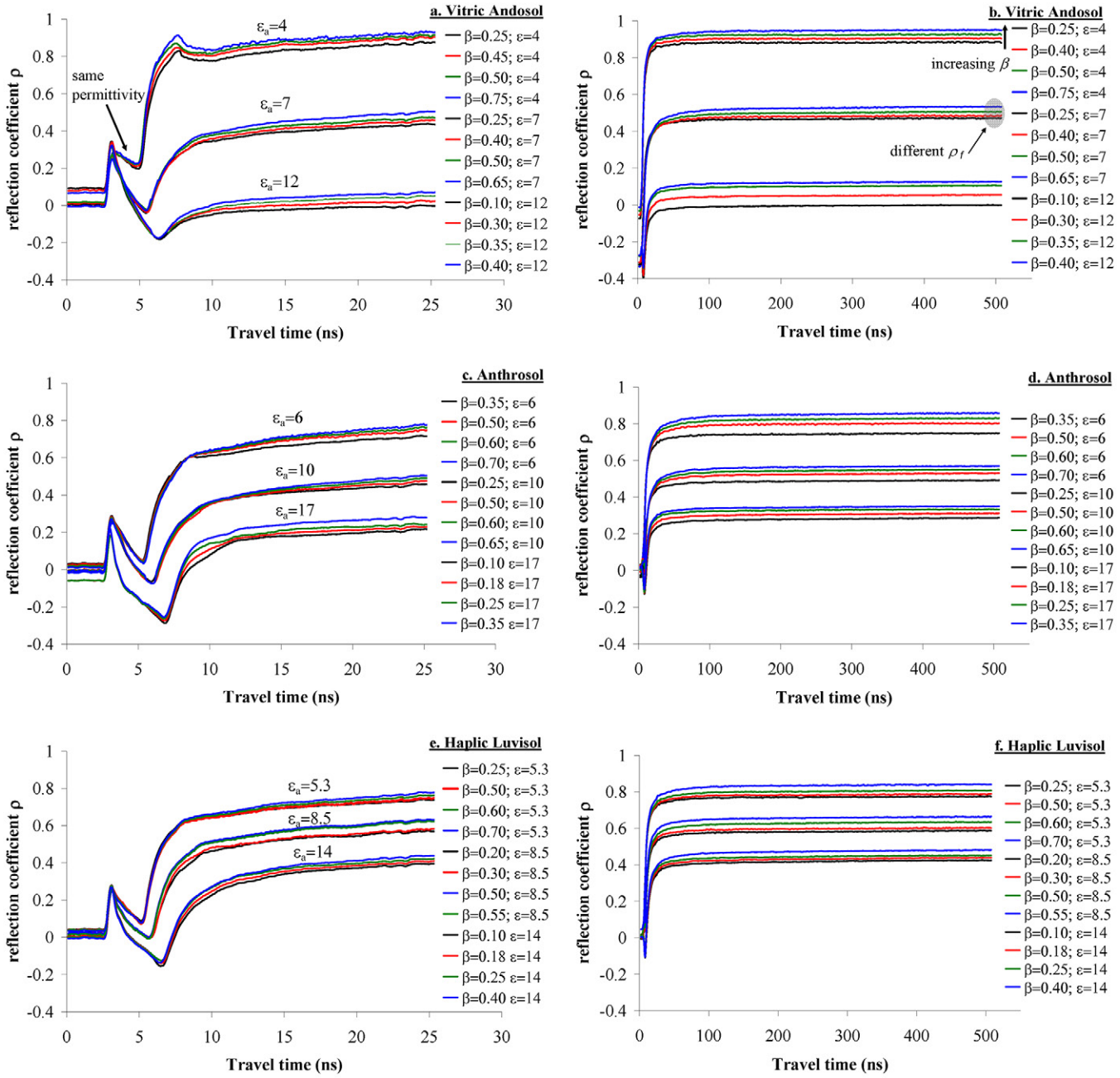

Fig. 3. Selected sample reflection time domain reflectivity waveforms measured in the three soils investigated, with reference to two observation windows (time t = 25.37 ns and t = 507.42 ns) and for different levels of contamination (β).

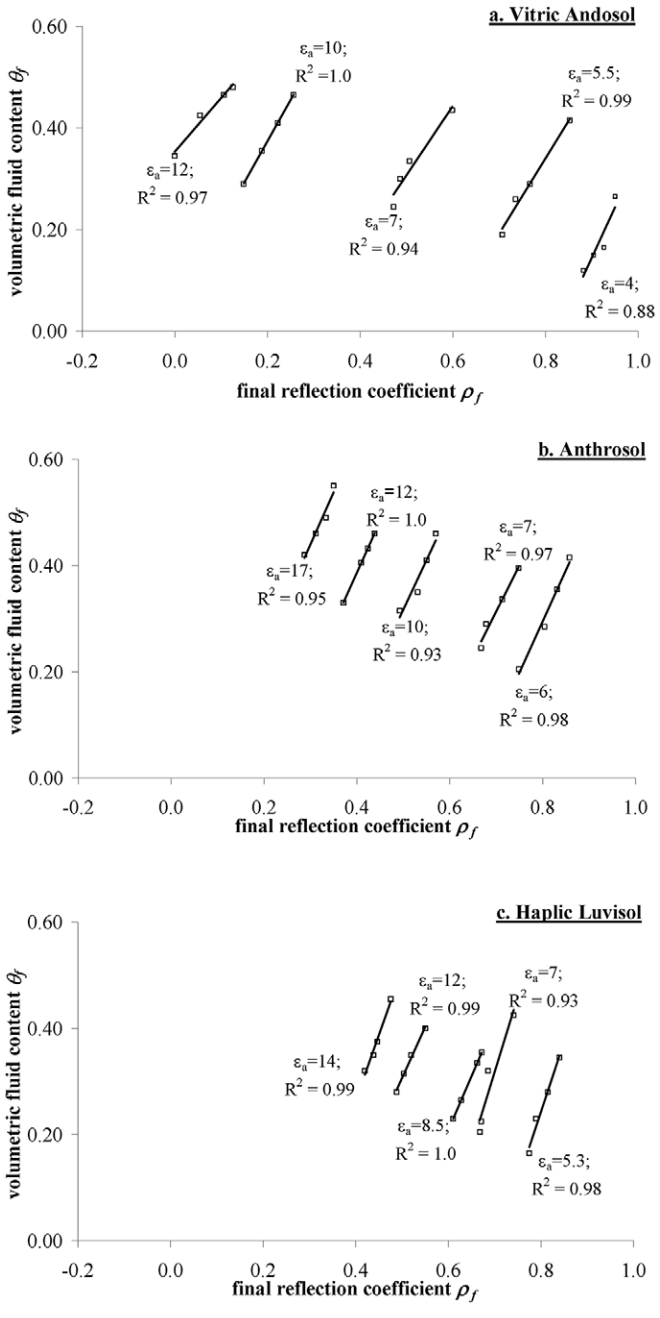

Fig. 4. Experimental relationship between volumetric fluid content (θ_f) and the final reflection coefficient (ρ_f), for constant apparent dielectric permittivity (ε_a): (a) Vitric Andosol, (b) Anthrosol, and (c) Haplic Luvisol.

to separate, and the magnitude of the reflection coefficient, ρ, for a given permittivity, ε_a, systematically increases with the NAPL content. Figures 3b, 3d, and 3f depict the same TDR waveforms as Fig. 3a, 3c, and 3e, extended to larger travel times to show that after multiple reflections, the distance between waveforms stabilizes and regularly increases with increasing NAPL content.

Figure 4 shows the experimental θ_f–ρ_f relationships obtained for different ε_a according to the procedure described above. The

Table 5. Estimated coefficients of the fluid volume (θ_f) vs. final reflection coefficient (ρ_f) relationship for all three soil types used.

Soil	a_c	b_1	b_2	b_3
Vitric Andosol	1.403	−0.0114	0.3632	−2.3952
Anthrosol	1.881	−0.0075	0.2717	−2.5578
Haplic Luvisol	2.423	−0.0040	0.1864	−2.5423

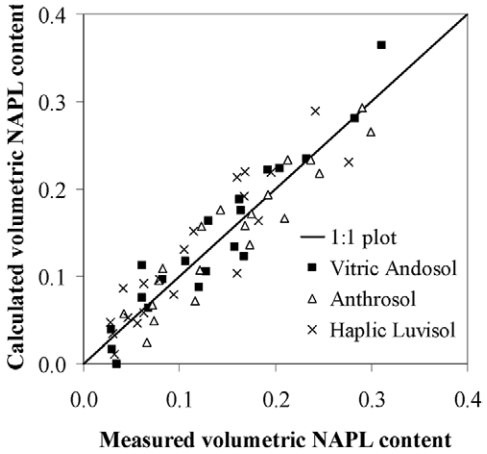

Fig. 5. Measured (Eq. [14]) vs. known volumetric nonaqueous-phase liquid (NAPL) content (θ_{NAPL}) of contaminated soils.

volumetric fluid content and the final reflection coefficient are highly linearly correlated, as indicated by the coefficient of determination R^2, which varies between 0.88 and 1.0 for the Vitric Andosol and between 0.93 and 1.0 for the Anthrosol and the Haplic Luvisol. Additionally, at first glance the slope of all the lines seems to be similar. An ANCOVA analysis performed at a significance level of 0.05 confirmed the parallelism among the θ_f–ρ_f regression lines. A common slope, a_c, of 1.403, 1.882, and 2.423 was found for the Vitric Andosol, Anthrosol, and Haplic Luvisol, respectively. This result suggests that, for a given soil, the slope of the θ_f–ρ_f regression lines might be identified at only one selected ε_a and thus the intercept is the only calibration parameter changing with ε_a. The complete data set of computed a_c, b_1, b_2, and b_3 coefficients for all the soils investigated is reported in Table 5.

Figure 5 shows the volumetric NAPL content computed from Eq. [14] and the known θ_{NAPL} content obtained from an independent data set specifically acquired for model validation. The trend line has $R^2 = 0.95$, meaning that the methodology proposed in this study has a very high precision.

Table 6 depicts the corresponding statistical indices for model performance evaluation, as well as the range of model applicability, which defines the limits of Eq. [14]. The statistical indices, calculated for each soil, show satisfactory agreement of the model predictions with the experimental data. The MBE and

Table 6. Range of model applicability in terms of the apparent dielectric permittivity (ε_a) and the mean bias error (MBE), model efficiency (EF), maximum absolute percentage error (ME), and mean absolute percentage error (MAE) statistical indices, referring to the measured and predicted (Eq. [14]) volumetric NAPL content.

Soil	Range of model applicability	MBE	EF	ME	MAE
				%	
Vitric Andosol	$4 < \varepsilon_a < 12$	−0.0049	0.99	5.3	2.3
Anthrosol	$6 < \varepsilon_a < 17$	0.0067	0.99	4.4	2.2
Haplic Luvisol	$5.3 < \varepsilon_a < 14$	−0.0107	0.96	5.6	2.8

EF are very close to 0 and 1, respectively, the ME is (among the soils) between 4.4 and 5.6%, and the MAE is approximately 2.5%. Considering the complexity of the modeled process, these results confirm the scientific reliability of the approach and its general applicability to determining volumetric NAPL content in real cases.

Conclusions

The present study aimed to develop a new methodological approach for electromagnetic characterization of NAPL-contaminated soils at the laboratory scale by means of a new α mixing model formulation, which was extended from two or three phases to four components for θ_{NAPL} quantification. The results of the methodology proposed, based on coupling the TDR technique with the α mixing model, are encouraging.

The dielectric permittivity, ε_a, and the asymptotic value of the reflection coefficient, ρ_f, were measured in the TDR megahertz frequency range on a sandy soil, a silty loam, and a loam soil contaminated with a corn oil considered as an NAPL contaminant. Different mixtures of water and oil in soils can result in TDR signals with the same travel time. Thus, analyzing the TDR waveforms only allows the presence of oil to be revealed qualitatively by, say, checking differences in dielectric permittivity and/or electrical conductivity, which can demonstrate in such a manner the presence of an NAPL contaminant in the soil. By contrast, further examination of the behavior of the signal after multiple reflections also permits the θ_{NAPL} to be identified. The proposed model provides a powerful tool for the NAPL estimate with an acceptable accuracy ($R^2 = 0.95$) once the α exponent of the dielectric mixing model has been determined. The empirical parameters (a_c, b_1, b_2, and b_3) of the θ_f–ρ_f relationship included in Eq. [14] are soil specific and thus have to be calibrated. What is important here is that, for a given soil, the slope a_c does not change with the dielectric permittivity, due to the parallelism observed in the experimental θ_f vs. ρ_f relationships derived among the different soils investigated.

The methodology proposed is an enhancement in NAPL detection in contaminated soils with regard to the main attempts proposed in the literature. However, there are the following intrinsic limitations: (i) θ_{NAPL} is strongly dependent on soil porosity, which must be constant; (ii) Eq. [14] holds only for low dispersive materials (otherwise the imaginary permittivity must be considered in the analysis); and (iii) Eq. [14] is applicable under the hypothesis that θ_w and θ_{NAPL} are uniformly distributed in the soil.

The approach requires additional experiments and data sets for model calibration in different pedological contexts, mainly to: (i) confirm the potential of the methodology developed; and (ii) fully explore the physical basis of the observed relationship between the NAPL content and TDR signal attenuation. Full field-scale tests should also be conducted to evaluate the performance of Eq. [14] under real field conditions.

References

Ajo-Franklin, J.B., J.T. Geller, and J.M. Harris. 2006. A survey of the geophysical properties of chlorinated DNAPLs. J. Appl. Geophys. 59:177–189. doi:10.1016/j.jappgeo.2005.10.002

Alharthi, A., J. Lange, and E. Whitaker. 1986. Immiscible fluid flow in porous media: Dielectric properties. J. Contam. Hydrol. 1:107–118. doi:10.1016/0169-7722(86)90010-0

Allison, L.E. 1965. Organic carbon. In: C.A. Black et al., editors, Methods of soil analysis. Part 2. Agron. Monogr. 9. ASA and SSSA, Madison, WI. p. 1367–1378. doi:10.2134/agronmonogr9.2.2ed.c39

Baker, J.M., and R.R. Allmaras. 1990. System for automating and multiplexing soil moisture measurement by time domain reflectometry. Soil Sci. Soc. Am. J. 54:1–6. doi:10.2136/sssaj1990.03615995005400010001x

Birchak, J.R., C.Z.G. Gardner, J.E. Hipp, and J.M. Victor. 1974. High dielectric constant microwave probes for sensing soil moisture. Proc. IEEE 62:93–98. doi:10.1109/PROC.1974.9388

Chenaf, D., and N. Amara. 2001. Time domain reflectometry for the characterization of diesel contaminated soils. In: Proceedings of the 2nd International Symposium and Workshop on Time Domain Reflectometry for Innovative Geotechnical Applications, Evanston, IL. 5–7 Sept. 2001. Northwestern Univ., Evanston, IL.

Comegna, A., A. Coppola, G. Dragonetti, G. Severino, A. Sommella, and A. Basile. 2013a. Dielectric properties of a tilled sandy volcanic-vesuvian soil with moderate andic features. Soil Tillage Res. 133:93–100. doi:10.1016/j.still.2013.06.003

Comegna, A., A. Coppola, G. Dragonetti, and A. Sommella. 2013b. Dielectric response of a variable saturated soil contaminated by non-aqueous phase liquids (NAPLs). Procedia Environ. Sci. 19:701–710. doi:10.1016/j.proenv.2013.06.079

Conover, W.T., and R.L. Iman. 1982. Analysis of covariance using the rank transformation. Biometrics 38:715–724. doi:10.2307/2530051

Coppola, A., G. Dragonetti, A. Comegna, N. Lamaddalena, B. Caushi, M.A. Haikal, and A. Basile. 2013. Measuring and modeling water content in stony soils. Soil Tillage Res. 128:9–22. doi:10.1016/j.still.2012.10.006

Dalton, F.N., W.N. Herkelrath, D.S. Rawlins, and J.D. Rhoades. 1984. Time-domain reflectometry: Simultaneous measurement of soil water content and electrical conductivity with a single probe. Science 224:989–990. doi:10.1126/science.224.4652.989

Day, P.R. 1965. Particle fractionation and particle-size analysis. In: C.A. Black et al., editors, Methods of soil analysis. Part 1. ASA and SSSA, Madison, WI. p. 545–567. doi:10.2134/agronmonogr9.1.c43

De Loor, G.P. 1954. Dielectric properties of heterogeneous mixtures. Appl. Sci. Res. 3:479–482. doi:10.1007/BF02919923

Dobson, M.C., F.T. Ulaby, M.T. Hallikainen, and M.A. El-Rayes. 1985. Microwave dielectric behavior of wet soil: II. Dielectric mixing models. IEEE Trans. Geosci. Remote Sens. GE-23:35–46. doi:10.1109/TGRS.1985.289498

Eckert, D.J. 1988. Soil pH. In: W.C. Dahnke, editor, Recommended chemical soil test procedures for the North Central Region. Bull. 221 (revised). North Dakota Agric. Exp. Stn., Fargo. p. 6–8.

Francisca, M., and M.A. Montoro. 2012. Measuring the dielectric properties of soil–organic mixtures using coaxial impedance dielectric reflectometry. J. Appl. Geophys. 80:101–109. doi:10.1016/j.jappgeo.2012.01.011

Francisca, M., and M.A. Montoro. 2014. Influence of particle size distribution and wettability on the displacement of LNAPL in saturated sandy soils. J. Environ. Eng. 141(6):04014091. doi:10.1061/(ASCE)EE.1943-7870.0000915

Gerhard, J.I., T. Pang, and B.H. Kueper. 2007. Time scales of DNAPL migration in sandy aquifers. Ground Water 45:147–157. doi:10.1111/j.1745-6584.2006.00269.x

Giese, K., and R. Tiemann. 1975. Determination of the complex permittivity from thin-sample time domain reflectometry: Improved analysis of the step response waveform. Adv. Mol. Relax. Processes 7:45–49. doi:10.1016/0001-8716(75)80013-7

Goovaerts, P., G. AvRuskin, J. Meliker, M. Slotnick, G. Jacquez, and J. Nriagu. 2005. Geostatistical modeling of the spatial variability of arsenic in groundwater of southeast Michigan. Water Resour. Res. 41:W07013. doi:10.1029/2004WR003705

Haridy, S.A., M. Persson, and R. Berndtsson. 2004. Estimation of LNAPL saturation in fine sand using time-domain reflectometry. Hydrol. Sci. J. 49:987–1000. doi:10.1623/hysj.49.6.987.55729

Hilhorst, M.A. 1998. Dielectric characterisation of soil. Ph.D. diss. Wageningen Agric. Univ., Wageningen, the Netherlands.

Huisman, J.A., S.S. Hubbard, J.D. Redman, and A.P. Annan. 2003. Measuring soil water content with ground penetrating radar: A review. Vadose Zone J. 2:476–491. doi:10.2136/vzj2003.4760

Illangasekare, H.T. 1998. Flow and entrapment of non-aqueous-phase fluids in heterogeneous soil formation. In: M.H. Selim and L. Ma, editors, Physical nonequilibrium in soils. Ann Arbor Press, Ann Arbor, MI. p. 417–435.

IUSS Working Group WRB. 2006. World reference base for soil resources 2006: A framework for international classification, correlation and communication. 2nd ed. World Soil Resour. Rep. 103. FAO, Rome.

Jung, S., V.P. Drnevich, and M.R. Abou Najm. 2013. New methodology for density and water content by time domain reflectometry. J. Geotech. Geoenviron. Eng. 139:659–670. doi:10.1061/(ASCE)GT.1943-5606.0000783

Jury, W.A., and R. Horton. 2004. Soil physics. John Wiley & Sons, Hoboken, NJ.

Kameyama, K., and T. Miyamoto. 2008. Measurement of solid phase permittivity for soils by time domain reflectometry. Eur. J. Soil Sci. 59:1253–1259. doi:10.1111/j.1365-2389.2008.01070.x

Knight, R. 2001. Ground penetrating radar for environmental applications. Annu. Rev. Earth Planet. Sci. 29:229–255. doi:10.1146/annurev.earth.29.1.229

Legates, D.R., and G.J. McCabe, Jr. 1999. Evaluating the use of "goodness-of-fit" measures in hydrologic and hydroclimatic model validation. Water Resour. Res. 35:233–241. doi:10.1029/1998WR900018

Mercer, J.W., and R.M. Cohen. 1990. A review of immiscible fluids in the subsurface: Properties, models, characterization, and remediation. J. Contam. Hydrol. 6:107–163. doi:10.1016/0169-7722(90)90043-G

Miller, J.J., and D. Curtin. 2006. Electrical conductivity and soluble ions. In: M.R. Carter and E.G. Gregorich, editors, Soil sampling and methods of analysis. 2nd ed. CRC Press, Boca Raton, FL. p. 1661–171. doi:10.1201/9781420005271.ch15

Mohamed, A.M.O. 2006. Principles and applications of time domain electrometry in geoenvironmental engineering. Dev. Arid Region Res. 5. CRC Press, Boca Raton, FL.

Mohamed, A.M.O., and R.A. Said. 2005. Detection of organic pollutants in sandy soils via TDR and eigendecomposition. J. Contam. Hydrol. 76:235–249. doi:10.1016/j.jconhyd.2004.09.002

Moroizumi, T., and Y. Sasaki. 2008. Estimating the nonaqueous-phase liquid content in saturated sandy soil using amplitude domain reflectometry. Soil Sci. Soc. Am. J. 72:1520–1526. doi:10.2136/sssaj2006.0212

Persson, M., and R. Berndtsson. 2002. Measuring nonaqueous phase liquid saturation in soil using time domain reflectometry. Water Resour. Res. 38(5). doi:10.1029/2001WR000523

Redman, J.D., and S.M. DeRyck. 1994. Monitoring non-aqueous phase liquids in the subsurface with multilevel time domain reflectometry probes. In: Proceedings of the Symposium on Time Domain Reflectometry in Environmental, Infrastructure, and Mining Applications, Evanston, IL. Spec. Publ. SP19-94. US Bur. of Mines, Washington, DC. p. 207–214.

Redman, J.D., B.H. Kueper, and A.P. Annan. 1991. Dielectric stratigraphy of a DNAPL spill and implications for detection with ground penetrating radar. In: Proceedings of the 5th National Outdoor Action Conference on Aquifer Restoration, Ground Water Monitoring, and Geophysical Methods, Las Vegas, NV. 13–16 May 1991. Natl. Water Well Assoc., Dublin, OH. p. 1017–1030.

Regalado, C.M., R. Munoz-Carpena, A.R. Socorro, and J.M. Hernandez-Moreno. 2003. Time domain reflectometry models as a tool to understand the dielectric response of volcanic soils. Geoderma 117:313–330. doi:10.1016/S0016-7061(03)00131-9

Rhoades, J.D., P.A.C. Raats, and R.J. Prather. 1976. Effects of liquid-phase electrical conductivity, water content, and surface conductivity on bulk soil electrical conductivity. Soil Sci. Soc. Am. J. 5:651–655.

Rinaldi, V.A., and F.M. Francisca. 2006. Removal of immiscible contaminants from sandy soils monitored by means of dielectric measurements. J. Environ. Eng. 132:931–939. doi:10.1061/(ASCE)0733-9372(2006)132:8(931)

Robinson, D.A., and S.P. Friedman. 2002. The effective permittivity of dense packing of glass beads, quartz sand and their mixtures immersed in different dielectric backgrounds. J. Non-Cryst. Solids 305:261–267. doi:10.1016/S0022-3093(02)01099-2

Roth, K., R. Shulin, H. Flühler, and W. Attinger. 1990. Calibration of time domain reflectometry for water content measurement using a composite dielectric approach. Water Resour. Res. 26:2267–2273.

Topp, G.C., J.L. Davis, and A.P. Annan. 1980. Electromagnetic determination of soil water content: Measurement in coaxial transmission lines. Water Resour. Res. 16:574–582. doi:10.1029/WR016i003p00574

van Dam, R.L., B. Borchers, and J.M.H. Hendrickx. 2005. Methods for prediction of soil dielectric properties: A review. Proc. SPIE 5794:188–197. doi:10.1117/12.602868

Zhan, L.T. Q.Y. Mu, Y.M. Chen, and R.P. Chen. 2013. Experimental study on applicability of using time-domain reflectometry to detect NAPLs contaminated sands. Sci. China Technol. Sci. 56:1534–1543. doi:10.1007/s11431-013-5211-8